



Cite this: *Chem. Commun.*, 2017, 53, 1619

Received 7th November 2016,  
Accepted 9th January 2017

DOI: 10.1039/c6cc08892a

www.rsc.org/chemcomm

# Accelerated room-temperature crystallization of ultrahigh-surface-area porous anatase titania by storing photogenerated electrons†

Juan Su,<sup>a</sup> Xiaoxin Zou,<sup>b</sup> Bingham Li,<sup>a</sup> Hui Chen,<sup>b</sup> Xinhao Li,<sup>c</sup> Qiuying Yu,<sup>c</sup> Qixi Mi<sup>\*a</sup> and Jie-Sheng Chen<sup>\*c</sup>

Room-temperature crystallization, a mild and energy-efficient process, shows important application potentials for developing functional materials. We significantly accelerated the crystallization of amorphous TiO<sub>2</sub> at room temperature by storing photogenerated electrons and the resulting porous anatase titania exhibits ultrahigh surface areas up to 736 m<sup>2</sup> g<sup>−1</sup>.

In recent years, considerable research efforts have been made for the development of mild chemical synthesis routes without energy-intensive processes to meet the requirement of green chemistry (eco-friendly and energy efficient) and prospective applications.<sup>1,2</sup> Furthermore, low- and room-temperature synthesis steps are particularly needed for the preparation of functional materials with specific structures. Compared with the energy-intensive approaches, mild synthesis routes would be helpful in maintaining some compositions, morphologies or structures, and thus beneficial for related properties and functions of materials.<sup>2</sup>

Porous titania is one of the most important synthetic functional semiconductors because of its excellent physical/chemical properties and large surface area.<sup>3–5</sup> The construction of pore channels conventionally involves a final thermal treatment at  $T \geq 400$  °C to remove the template/surfactants/remnants. In addition, in most cases, an energy-intensive treatment process is needed to improve their crystallinity, *e.g.* calcination, solvo/hydrothermal, microwave treatment, *etc.* (Table S1 in the ESI†). Recently, we reported the spontaneous crystallization of porous amorphous TiO<sub>2</sub> (Am-TiO<sub>2</sub>) to anatase titania with a large surface area and excellent photocatalytic performance, at room temperature in 80 days.<sup>6</sup>

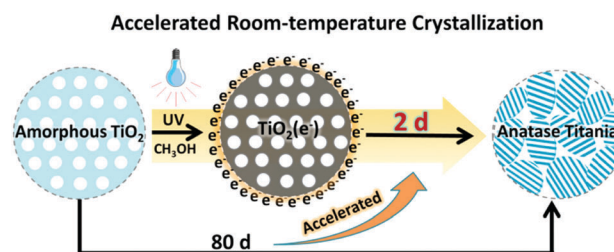


Fig. 1 Schematic representation of the accelerated room-temperature crystallization from Am-TiO<sub>2</sub> to anatase titania. Crystallization time is reduced from 80 d to 2 d by storing  $e^-$ .

The development of such a room-temperature crystallization process without any solvent, additive, or catalyst is significant for exploring green and energy-efficient chemical synthesis. Nonetheless, the acceleration of the process of room-temperature crystallization is desirable for the research and application of such a mild synthetic route in the development of functional materials.

Herein, we report that the room-temperature crystallization from amorphous to anatase porous titania can be significantly accelerated by storing photogenerated electrons ( $e^-$ ) (Fig. 1). In most cases,  $e^-$  acts as an intermediate with a limited amount and short lifetime. Recently, we have successfully stored abundant  $e^-$  on the surface of porous titania in the form of Ti<sup>3+</sup> through photochemical reduction.<sup>7</sup> The stored  $e^-$  exhibited unique applications, such as chemoselective hydrogenation of nitroarene and room-temperature ferromagnetism.<sup>7–9</sup> A mechanism for the accelerated room-temperature crystallization is also discussed in this work.

Porous Am-TiO<sub>2</sub> was synthesized photochemically according to our previous report.<sup>7</sup> After 30 min of UV-light irradiation, abundant  $e^-$  were stored on the surface of porous Am-TiO<sub>2</sub> suspended in aqueous methanol (methanol as a sacrificial agent of photogenerated holes improves the accumulation of photogenerated electrons on Am-TiO<sub>2</sub><sup>7</sup>). A self-made reactor with a volume of 3.5 L was applied to provide irradiation, constant cooling and stirring in a lightproof enclosure as shown in Fig. S1 (ESI†). We can carry out the storage of  $e^-$  in

<sup>a</sup> School of Physical Science and Technology, ShanghaiTech University, Shanghai 201210, China. E-mail: miqx@shanghaitech.edu.cn

<sup>b</sup> State Key Laboratory of Inorganic Synthesis and Preparative Chemistry, Jilin University, Changchun 130012, China

<sup>c</sup> School of Chemistry and Chemical Engineering, Shanghai Jiao Tong University, Shanghai 200240, China. E-mail: chemcj@sjtu.edu.cn

† Electronic supplementary information (ESI) available: Experimental details and supporting results. See DOI: 10.1039/c6cc08892a



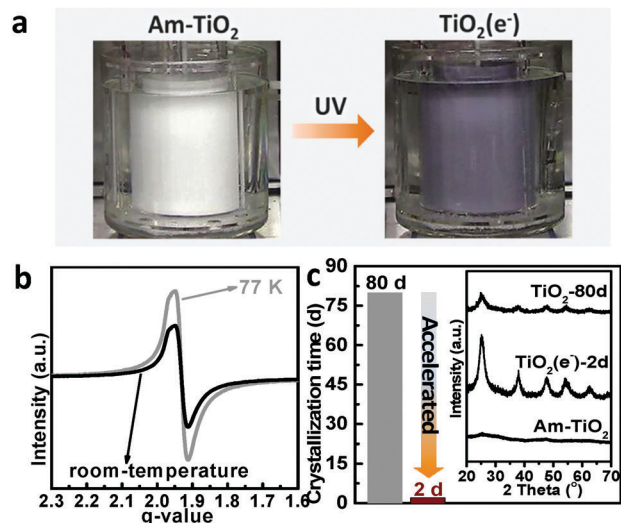


Fig. 2 (a) Photographs of Am-TiO<sub>2</sub> and TiO<sub>2</sub>(e<sup>-</sup>) in the photochemical reactor. (b) The electron paramagnetic resonance (EPR) spectra of TiO<sub>2</sub>(e<sup>-</sup>) at 77 K and room-temperature. (c) Crystallization time of TiO<sub>2</sub>-80d (grey) and TiO<sub>2</sub>(e<sup>-</sup>)-2d (red); inset: the powder X-ray diffraction (XRD) patterns of Am-TiO<sub>2</sub>, TiO<sub>2</sub>(e<sup>-</sup>)-2d, and TiO<sub>2</sub>-80d.

at least 140 g titania sample each time. As e<sup>-</sup> is stored on the titania surfaces (denoted as TiO<sub>2</sub>(e<sup>-</sup>)), the color of the reaction mixture gradually turned from white to dark gray (Fig. 2a, Movie 1 in the ESI†), indicating that e<sup>-</sup> are trapped by Ti<sup>4+</sup> ions and then stored in the form of Ti<sup>3+</sup> ions. A characteristic Ti<sup>3+</sup> signal at  $g = 1.948$  was detected in the electron paramagnetic resonance (EPR) spectrum of TiO<sub>2</sub>(e<sup>-</sup>) (Fig. 2b).<sup>7</sup> Subsequently, TiO<sub>2</sub>(e<sup>-</sup>) was preserved for 2, 5, and 40 days, and the washed and dried samples (surface Ti<sup>3+</sup>/e<sup>-</sup> were oxidized by O<sub>2</sub> during washing and drying in air, Fig. S2 in the ESI†) were denoted as TiO<sub>2</sub>(e<sup>-</sup>)-2d, TiO<sub>2</sub>(e<sup>-</sup>)-5d, and TiO<sub>2</sub>(e<sup>-</sup>)-40d, respectively. By contrast, the samples crystallized in air at room temperature, including TiO<sub>2</sub>-80d and TiO<sub>2</sub>-300d, were also synthesized according to the previous method.<sup>6</sup>

As shown in Fig. 2c, TiO<sub>2</sub>(e<sup>-</sup>)-2d began to crystallize after 2 days, which was significantly accelerated compared with TiO<sub>2</sub>-80d (began to crystallize after 80 days). The inset in Fig. 2c shows the powder X-ray diffraction (XRD) patterns of Am-TiO<sub>2</sub>, TiO<sub>2</sub>(e<sup>-</sup>)-2d and TiO<sub>2</sub>-80d. In contrast to Am-TiO<sub>2</sub> with no observable XRD peaks, both of TiO<sub>2</sub>(e<sup>-</sup>)-2d and TiO<sub>2</sub>-80d show a set of characteristic peaks of anatase titania without any impurity phase after crystallization at room temperature. Although the crystallization time of TiO<sub>2</sub>(e<sup>-</sup>)-2d is one-fortieth of that of TiO<sub>2</sub>-80d, TiO<sub>2</sub>(e<sup>-</sup>)-2d shows higher crystallinity. The high crystallinity of TiO<sub>2</sub>(e<sup>-</sup>)-2d can be further confirmed by high-resolution transmission electron microscopy (HR-TEM, Fig. S3 in the ESI†) and selected-area electron diffraction (SAED) patterns (Fig. S4 in the ESI†). The lattice spacing 0.35, 0.24, and 0.19 nm observed by HR-TEM correspond to the (101), (004) and (200) crystal planes of anatase, respectively. The diffraction rings observed in the SAED pattern also agree with these results.

In addition, N<sub>2</sub>-adsorption measurements reveal that both of TiO<sub>2</sub>(e<sup>-</sup>)-2d and TiO<sub>2</sub>-80d inherit the highly porous texture

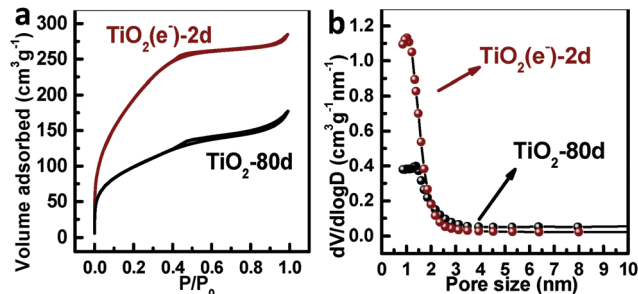


Fig. 3 (a) N<sub>2</sub> adsorption-desorption isotherms and (b) pore size distribution of TiO<sub>2</sub>(e<sup>-</sup>)-2d and TiO<sub>2</sub>-80d.

from Am-TiO<sub>2</sub> (Fig. 3). In particular, to our knowledge, TiO<sub>2</sub>(e<sup>-</sup>)-2d possesses the maximum surface area (736 m<sup>2</sup> g<sup>-1</sup>) of porous anatase titania reported so far, a value nearly twice that of TiO<sub>2</sub>-80d (400 m<sup>2</sup> g<sup>-1</sup>) (Table S1 in the ESI†). It is known that the crystallization process tends to impart tightness and regularity to particle packing, which would increase both the number and size of pores in a material. TiO<sub>2</sub>(e<sup>-</sup>)-2d from the accelerated crystallization possesses more pores and smaller pore sizes, which result in a larger Brunauer-Emmett-Teller (BET) surface area compared with TiO<sub>2</sub>-80d. As anticipated, after a longer crystallization time than that of TiO<sub>2</sub>(e<sup>-</sup>)-2d, TiO<sub>2</sub>(e<sup>-</sup>)-5d displays a slightly smaller BET surface area (689 m<sup>2</sup> g<sup>-1</sup>) and larger pore sizes (Fig. S5 and Table S2 in the ESI†). Therefore, the storage of e<sup>-</sup> during the room-temperature crystallization process of titania not only significantly reduces the reaction time, but also contributes to the ultrahigh surface area of the as-obtained porous anatase.

As shown in Fig. 4a, we compared the crystallization curves of titania with and without e<sup>-</sup> based on the evolution of XRD patterns<sup>10</sup> (Fig. S6 and S7 in the ESI†). It was revealed that the crystallinity of titania increased at distinct rates, and both of the nucleation and crystal growth rates were accelerated by the storage of e<sup>-</sup>. In our synthetic process of anatase (Fig. S8 in the ESI†), titanium glycolate (TG) as the precursor of Am-TiO<sub>2</sub> is constructed by infinite chains, which consist of edge-sharing TiO<sub>6</sub> octahedra and organic ligands.<sup>11</sup> After removing the organic ligands by UV irradiation, TG was transformed into Am-TiO<sub>2</sub>, which consists of randomly arranged TiO<sub>6</sub> octahedra

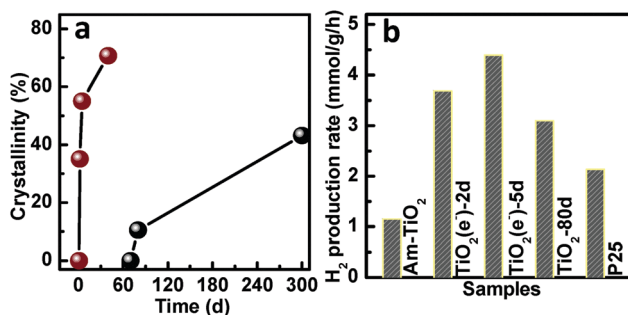


Fig. 4 (a) Room-temperature crystallization curves of titania with (red) and without (black) e<sup>-</sup>. (b) Comparison of H<sub>2</sub> production rates. Reaction conditions: 50 mg catalyst; 1 wt% Pt loading; aqueous methanol solution (50 vol%, 100 mL); and 300 W Xe lamp as a light source.



or their edge-shared fragments (Fig. S9 in the ESI†).<sup>6</sup> An orderly rearrangement and connection of octahedral  $\text{TiO}_6$  units would produce anatase titania (containing ordered edge/corner-sharing  $\text{TiO}_6$  octahedra). Infrared spectroscopy (Fig. S10 in the ESI†), thermogravimetric analysis (Fig. S11 in the ESI†), and elemental analysis (Table S3 in the ESI†) suggested that Am- $\text{TiO}_2$ ,  $\text{TiO}_2(\text{e}^-)$ -2d and  $\text{TiO}_2(\text{e}^-)$ -5d contained ethylene glycol,<sup>12</sup> which gradually decreased as the crystallization time increased from Am- $\text{TiO}_2$  to  $\text{TiO}_2(\text{e}^-)$ -2d, and then to  $\text{TiO}_2(\text{e}^-)$ -5d. The residual ethylene glycol remaining after the TG transformation may hinder the rearrangement and interconnection of the  $\text{TiO}_6$  octahedra in Am- $\text{TiO}_2$ . Therefore, we propose that the storage of  $\text{e}^-$  facilitates the removal of residual ethylene glycol from  $\text{TiO}_6$  octahedra and thus accelerates the room-temperature crystallization of porous titania. This is because the storage of  $\text{e}^-$  turns some  $\text{Ti}^{4+}$  sites into  $\text{Ti}^{3+}$ , and weakens the Ti–O bond between titania and ethylene glycol (Fig. S8, I, in the ESI†). In addition, we demonstrated that a proton was attached to the surface oxygen combined with an  $\text{e}^-$  stored on the neighboring  $\text{Ti}^{3+}$ ,<sup>7</sup> which is consistent with the concept “proton-coupled electron transfer (PCET)” proposed by Schrauben *et al.*<sup>13</sup> These protonated surfaces would be easily combined with the hydroxyl group of other  $\text{TiO}_6$  octahedra in the vicinity.<sup>14</sup> Thus, after eliminating a  $\text{H}_2\text{O}$  molecule, a bridging oxygen bond (Ti–O–Ti) would form between two neighbouring  $\text{TiO}_6$  octahedra, which favors the connection of  $\text{TiO}_6$  octahedra to form anatase (Fig. S8, II, in the ESI†). In addition, we flew oxygen through  $\text{TiO}_2(\text{e}^-)$  and the resulting sample without  $\text{e}^-$  could not crystallize in the same solvent system even after 40 days. This observation confirmed the key role of  $\text{e}^-$  rather than the solvent in accelerating the room-temperature crystallization process.

It was previously demonstrated that  $\text{TiO}_2$ -80d was an efficient photocatalyst for  $\text{H}_2$  evolution under UV light, due to its large surface area and anatase structure.<sup>6</sup> Photocatalytic  $\text{H}_2$  production performance of the samples synthesized *via* accelerated room-temperature crystallization was also investigated (see the ESI† for details). In a control experiment, there was no  $\text{H}_2$  detected in the absence of the photocatalyst or light. It should be noted that  $\text{e}^-$  was not stored in the catalyst during photocatalysis, but rapidly transferred to the loaded Pt co-catalyst and then reacted with  $\text{H}_2\text{O}$ . Fig. 4b presents the comparison of photocatalytic  $\text{H}_2$  evolution rates of Am- $\text{TiO}_2$ ,  $\text{TiO}_2$ -80d,  $\text{TiO}_2(\text{e}^-)$ -2d,  $\text{TiO}_2(\text{e}^-)$ -5d and P25 (a benchmark photocatalyst).  $\text{TiO}_2$ -80d,  $\text{TiO}_2(\text{e}^-)$ -2d, and  $\text{TiO}_2(\text{e}^-)$ -5d show higher  $\text{H}_2$  evolution rates than those of P25 and Am- $\text{TiO}_2$ , due to their larger surface areas and anatase structure resulting from the mild room-temperature crystallization process. Compared with  $\text{TiO}_2$ -80d,  $\text{TiO}_2(\text{e}^-)$ -2d and  $\text{TiO}_2(\text{e}^-)$ -5d exhibited enhanced photocatalytic activities and higher photogenerated charge separation efficiency (Fig. S12 in the ESI†). There was no obvious difference of absorption onset or band gap among  $\text{TiO}_2$ -80d,  $\text{TiO}_2(\text{e}^-)$ -2d and  $\text{TiO}_2(\text{e}^-)$ -5d (Fig. S13 in the ESI†). The enhanced photocatalytic performance should be mainly attributed to their much larger surface area and higher crystallinity.  $\text{TiO}_2(\text{e}^-)$ -5d was proved to be the sample with the highest photogenerated charge separation efficiency and photocatalytic activity. This is mainly due to its high crystallinity, although its BET surface area is

somewhat smaller than that of  $\text{TiO}_2(\text{e}^-)$ -2d. In addition, 10 cycles of photocatalytic  $\text{H}_2$  evolution were performed over  $\text{TiO}_2(\text{e}^-)$ -2d, and excellent stability was observed with no obvious loss of catalytic activity (Fig. S14 in the ESI†) and no change in the crystal structure (Fig. S15 in the ESI†).

In this work, a technology for storing photogenerated electrons is for the first time applied for accelerating the amorphous–anatase phase transition of porous titania materials with large surface areas at room temperature. Thanks to the storage of  $\text{e}^-$ , the reaction time of such a mild room-temperature crystallization process was drastically reduced from 80 to 2 days. The as-prepared porous anatase titania materials possess ultrahigh surface areas (up to  $736 \text{ m}^2 \text{ g}^{-1}$ ) and high photocatalytic activity. Such a facile process permits easy scale-up and is promising for wide applications in both fundamental research and industrial productions.

This work was financially supported by the National Natural Science Foundation of China (21403140 and 21403141). We thank Dechun Qiu and Yi Zhang for their support to this work.

## Notes and references

- 1 F. Cheng, J. Shen, B. Peng, Y. Pan, Z. Tao and J. Chen, *Nat. Chem.*, 2011, **3**, 79; J. Cravillon, S. Münzer, S.-J. Lohmeier, A. Feldhoff, K. Huber and M. Wiebcke, *Chem. Mater.*, 2009, **21**, 1410; Y. Zhou and M. Antonietti, *J. Am. Chem. Soc.*, 2003, **125**, 14960.
- 2 D. Zhang, T. Yoshida, T. Oekermann, K. Furuta and H. Minoura, *Adv. Funct. Mater.*, 2006, **16**, 1228; X. Liu, Y. Luo, H. Li, Y. Fan, Z. Yu, Y. Lin, L. Chen and Q. Meng, *Chem. Commun.*, 2007, 2847; S. Ren, M. J. Bojdy, R. Dawson, A. Laybourn, Y. Z. Khimyak, D. J. Adams and A. I. Cooper, *Adv. Mater.*, 2012, **24**, 2357; S. H. Sun, D. Q. Yang, D. Villers, G. X. Zhang, E. Sacher and J. P. Dodelet, *Adv. Mater.*, 2008, **20**, 571.
- 3 W. Li, Z. Wu, J. Wang, A. A. Elzatahy and D. Zhao, *Chem. Mater.*, 2014, **26**, 287; A. A. Ismail, D. W. Bahnemann, L. Robben, V. Yarovyi and M. Wark, *Chem. Mater.*, 2010, **22**, 108; T. Brezesinski, J. Wang, J. Polleux, B. Dunn and S. H. Tolbert, *J. Am. Chem. Soc.*, 2009, **131**, 1802; J. Zhao, P. Xu, Y. Li, J. Wu, J. Xue, Q. Zhu, X. Lu and W. Ni, *Nanoscale*, 2016, **8**, 5417.
- 4 J. Su, X.-X. Zou, Y.-C. Zou, G.-D. Li, P.-P. Wang and J.-S. Chen, *Inorg. Chem.*, 2013, **52**, 5924.
- 5 G. J. A. A. Soler-Illia, C. Sanchez, B. Lebean and J. Patarin, *Chem. Rev.*, 2002, **102**, 4093; W. Y. Dong, Y. J. Sun, C. W. Lee, W. M. Hua, X. C. Lu, Y. F. Shi, S. C. Zhang, J. M. Chen and D. Y. Zhao, *J. Am. Chem. Soc.*, 2007, **129**, 13894; D. L. Li, H. S. Zhou and I. Honma, *Nat. Mater.*, 2004, **3**, 65; S. Y. Choi, M. Mamak, N. Coombs, N. Chopra and G. A. Ozin, *Adv. Funct. Mater.*, 2004, **14**, 335.
- 6 J. Su, X. Zou, G.-D. Li, Y.-M. Jiang, Y. Cao, J. Zhao and J.-S. Chen, *Chem. Commun.*, 2013, **49**, 8217.
- 7 X. X. Zou, G. D. Li, K. X. Wang, L. Li, J. Su and J. S. Chen, *Chem. Commun.*, 2010, **46**, 2112; J. Su, X.-X. Zou, G.-D. Li, L. Li, J. Zhao and J.-S. Chen, *Chem. Commun.*, 2012, **48**, 9032.
- 8 X. X. Zou, G. D. Li, Y. N. Wang, J. Zhao, C. Yan, M. Y. Guo, L. Li and J. S. Chen, *Chem. Commun.*, 2011, **47**, 1066.
- 9 J. Su, X. Zou and J.-S. Chen, *RSC Adv.*, 2014, **4**, 13979.
- 10 G. Feng, P. Cheng, W. Yan, M. Boronat, X. Li, J.-H. Su, J. Wang, Y. Li, A. Corma, R. Xu and J. Yu, *Science*, 2016, **351**, 1188.
- 11 X. X. Zou, G. D. Li, M. Y. Guo, X. H. Li, D. P. Liu, J. Su and J. S. Chen, *Chem. – Eur. J.*, 2008, **14**, 11123; D. Wang, R. Yu, N. Kumada and N. Kinomura, *Chem. Mater.*, 1999, **11**, 2008.
- 12 P. Liu, Y. Zhao, R. Qin, S. Mo, G. Chen, L. Gu, D. M. Chevrier, P. Zhang, Q. Guo, D. Zang, B. Wu, G. Fu and N. Zheng, *Science*, 2016, **352**, 797.
- 13 J. N. Schrauben, R. Hayoun, C. N. Valdez, M. Braten, L. Fridley and J. M. Mayer, *Science*, 2012, **336**, 1298.
- 14 H. Yin, Y. Wada, T. Kitamura, S. Kambe, S. Murasawa, H. Mori, T. Sakata and S. Yanagida, *J. Mater. Chem.*, 2001, **11**, 1694.

